Themodynamic and Transport Properties of Intermediate States of the Photocyclic Reaction of Photoactive Yellow Protein

Kan Takeshita,[‡] Yasushi Imamoto,[§] Mikio Kataoka,[§] Fumio Tokunaga,[||] and Masahide Terazima*[,‡]

Department of Chemistry, Graduate School of Science, Kyoto University, Kyoto 606-8502, Japan, Graduate School of Materials Science, Nara Institute of Science and Technology (NAIST), Nara 630-0101, Japan, and Department of Earth and Space Science, Graduate School of Science, Osaka University, Toyonaka, Osaka 560-0043, Japan

Received May 22, 2001; Revised Manuscript Received January 15, 2002

ABSTRACT: Themodynamic and transport properties of intermediate states of the photocyclic reaction of photoactive yellow protein (PYP) were studied by a combination of the pulsed laser-induced transient grating (TG), transient lens (TrL), and photoacoustic (PA) spectroscopies from tens of nanoseconds to hundreds of milliseconds. The diffusion coefficients (*D*) of PYP in the ground state (pG) and of the second intermediate state (pB) were determined by the TG analysis, and it was found that *D* of pG is about 1.2 times larger than *D* of pB. At the same time, *D* at various denatured conditions were measured using guanidine hydrochloride as the denaturant. *D* of completely unfolded protein is about 0.4 times that of the native form. The enthalpy of pB is estimated to be 60 kJ/mol by the TrL method with an assumption that the volume change of pB is not sensitive to the temperature. Since the enthalpy of the first intermediate state (pR) is as high as 160 kJ/mol, it implies that most of the photon energy is stored as the strain of the protein in pR, and this may be the driving force for the successive reaction to pB. From the temperature dependence of the volume change, the difference in the thermal expansion coefficients between pG and pR was calculated. All of the characteristic features of PYP, the negative volume change, the larger thermal expansion coefficient, and the slower diffusion process, indicate that the intermediate pR and pB are reasonably interpreted in terms of the unfolded (loosened) protein structure.

The thermodynamic properties (enthalpy, thermal expansion coefficient, compressibility, partial molar volume, etc.) as well as the transport property (diffusion coefficient) of proteins are of fundamental importance to understand the structural fluctuation and the dynamics of protein molecules. Indeed, much thermodynamic data obtained under various conditions of proteins have been accumulated so far. On the basis of these data, the characteristic features of not only the native state but also the unfolded state of proteins have been studied, and some general features have been elucidated. The traditional techniques that can access these quantities are certainly useful and powerful to characterize the proteins. However, a serious limitation inherent in the traditional techniques is that they are applicable only to steady-state protein structures. Knowledge of these properties of time-dependent or unstable (intermediate) species during biological reactions is very limited, which prevents us from using the compiled data to characterize the intermediate structures of proteins. It is most desirable to develop and use a method that can measure these properties in the time domain so that reaction intermediates can be characterized in a similar way.

The only technique we had so far for the measurement of the enthalpy change (ΔH) and the partial molar volume change (ΔV) of an irreversible reaction is the pulsed laser-induced photoacoustic (PA)[1] method that detects the pressure wave induced by the light irradiation (*1*−*3*). Because of its unique capability, this method has been applied to many reaction systems (*4*−*6*). However, even using this method, it is not possible to separate the volume and the energy contributions completely without any assumption. On the other hand, one of the authors (*7*, *8*) has already demonstrated for several simple chemical systems that a hybrid technique combining the laser-induced transient grating (TG) and the laser-induced photoacoustic (PA) techniques can be used to separate these contributions without any assumption; that is, this technique allows us to measure the enthalpy and volume changes in the time domain without performing temperature- or pressure-dependent measurement.

The transport property is another important factor for understanding the role of the protein conformation and stability. However, a measurement of the diffusion coefficient (*D*) has been also very difficult or almost impossible for transient species by the traditional techniques. The transport property of unstable intermediate biological molecules has not been elucidated at all so far. In this respect, again, the TG method was proven to be a powerful technique (*9*−*12*). *D* can be determined by a measurement which requires only 10 μs to milliseconds, so that *D* of a short-lived state during this time range can be studied. Thanks to these new

* Corresponding author. Tel: +81-75-753-4026. Fax: +81-75-753-4000. E-mail: mterazima@kuchem.kyoto-u.ac.jp.
[‡] Kyoto University.
[§] Nara Institute of Science and Technology.
[||] Osaka University.

[1] Abbreviations: BCP, bromocresol purple; CD, circular dichroism; *D*, diffusion coefficient; GdnHCl, guanidine hydrochloride; PA, photoacoustic; PYP, photoactive yellow protein; TG, transient grating; TrL, transient lens.

10.1021/bi0110600 CCC: $22.00
Published on Web 02/06/2002

developments, we are now able to access the thermodynamic properties and the transport property of unstable intermediate species of proteins during a biological reaction. As the first step along this approach, in this paper, we report a time-resolved study of energies and volume changes as well as the diffusion coefficients of intermediate species during the photocyclic reaction of photoactive yellow protein (PYP).

Interest in the photophysical and photochemical processes of PYP is rapidly increasing recently, because it is a simple model for studies of the signal transmitting system. PYP is a relatively new protein isolated from the purple sulfur bacterium *Ectothiorhodospira halophila* (*13*). It is considered to possess a function of a blue light photoreceptor for a negative phototactic response (*14*). It is a relatively small (14 kDa) water-soluble protein, and the protein structure was determined by X-ray crystallography in 1.4 Å resolution (*15*). The chromophore of PYP is *p*-coumaric acid (4-hydroxycinnamic acid) covalently bound to the side chain of Cys 69 via a thioester linkage (*16*, *17*). After photoexcitation, PYP undergoes a complete photocycle triggered by the photoisomerization of this chromophore. The photocyclic reaction has been a subject of intensive studies experimentally and theoretically (*18*, *19*). Upon flash excitation of the chromophore, the ground state (pG, $\lambda_{max} = 446$ nm) is converted into a red-shifted intermediate (pR, $\lambda_{max} = 465$ nm) in less than 2 ns (*19*). Subsequently, pR decays in a submillisecond time scale into a blue-shifted intermediate (pB, $\lambda_{max} = 355$ nm), which returns to pG in a subsecond time scale (*18*−*20*). Soon after the protein structure was revealed by X-ray crystallography (*15*, *16*), the time-resolved X-ray scattering experiments were performed (*21*, *22*). According to these studies, the structural change after light activation is localized near the chromophore. It revealed that the pR state possesses the cis conformation of the chromophore and that the process of trans to cis isomerization is accompanied by the specific formation of new hydrogen bonds. In the pB state, the phenolic oxygen of the chromophore moves from the hydrophobic core of protein to become solvent-exposed and protonated (*21*). However, these structural changes were questioned recently by the studies using NMR spectroscopy (*23*, *24*) and IR spectroscopy (*25*) in solution. These studies show that the dynamics of PYP in solution is more global, extending to the whole protein structure.

Previously, analyzing the TG signal in the 1−20 μs time scale, we preliminarily reported that the volume change (ΔV) for pG → pR is negative and the absolute value of ΔV increases with decreasing temperature (*26*). Here we report the full analysis of the TG signal from a few hundred nanoseconds to tens of milliseconds. Together, the enthalpy change to the second intermediate is also estimated using the transient lens (TrL) method with an assumption that the volume change to the pB state is not sensitive to the temperature. Although this assumption should be verified in the future, the obtained enthalpy of the pB state may be used for a preliminary discussion. Furthermore, we found that the D value of pB is about 0.8 times larger than that of the pG state. By measuring D of PYP denatured by guanidine hydrochloride, the smaller D is interpreted in terms of the unfolded nature of pB, and the extent of the unfolding in the pB state is estimated. The temperature-dependent ΔV is interpreted in terms of the larger thermal expansion coefficient of pR compared with that of pG. On the basis of the compiled data on the partial molar volume of native and unfolded states of proteins so far obtained, we suggest that all of these data indicate the partially unfolded nature of pR as well as pB.

EXPERIMENTAL PROCEDURES

Sample Preparation. PYP was prepared as reported previously (*27*). PYP was dissolved in 10 mM Tris-HCl (pH = 8.0) with 1 mM PMSF (phenylmethanesulfonyl fluoride). BCP (bromocresol purple) was used as a calorimetric reference. Concentrations of the sample and reference were adjusted so that the absorbances in the cell were the same at the excitation wavelength. Absorbance was about 0.7−1.0 in each experiment.

Apparatus. The details of the TG setup have been described previously (*9*, *26*). A TrL signal was measured with the same excitation pulse, probe light, and detection system as used in the TG measurement (*28*, *29*). The excitation beam was slightly focused by a lens with a focal length of 20 cm. The probe beam was brought into the sample collinearly with the pump beam. The probe beam after the sample was expanded by a concave lens, and the TrL signal was detected as a light intensity change through a pinhole. The excitation light was removed by an optical filter.

For a PA measurement, the sample was excited by a dye laser light, and the created pressure wave was detected by a piezoelectric transducer as described previously (*30*). The signal was directly recorded on a digital oscilloscope and averaged about 100−300 times.

A transient absorption signal was detected after photoexcitation with the dye laser pulse. A probe light (476 nm line of Ar^+ laser) was made nearly collinear to the excitation beam. The intensity change of the probe light was detected by a photomultiplier and averaged by a computer system.

The temperature of the sample was controlled by flowing methanol from a thermostatic bath around a sample holder. The temperature of the sample was measured with a thermocouple and a voltammeter.

Analysis. The procedure for the analysis of the TG and PA signals was reported previously (*7*, *8*, *26*, *31*). Here, we briefly summarize the TrL method.

In the TrL method, a sample is excited with a pump beam having a spatially Gaussian form. Under this condition, the profile of the concentration of the excited-state molecules should be the same Gaussian. If the absorptive change at the probe wavelength is negligible (this condition is satisfied for the PYP system probed at 633 nm), the signal intensity is proportional to the refractive index change. The refractive index change consists of the following three components: (1) contribution of the released heat (δn_{th}, thermal lens), (2) difference in the molecular refractive index between the reactant and products due to the change of the absorption spectrum (δn_{pop}, population lens), and (3) change in the density caused by the reaction volume change (δn_v, volume lens).

We often call the sum of δn_{pop} and δn_v the species lens (δn_{spe}), because the time profiles of δn_{pop} and δn_v are identical in most cases. If the refractive index changes by the several causes described above, the spatial profile of this change should have a Gaussian shape, too. At the central part, the

Gaussian profile of the refractive index acts as a lens to expand (or focus) another light beam passing through this region. The expansion (or focusing) of the light beam can be detected as a change in the light density through a pinhole placed at a far field.

The TrL signal intensity (I_{TrL}) is given by

$$I_{TrL}(t) = \alpha'[\delta n_{th}(t) + \delta n_{spe}(t)] \quad (1)$$

where α' is a proportional coefficient. The magnitude of the thermal lens is given by (*7*, *8*)

$$\delta n_{th} = \frac{dn}{dT}\frac{h\nu\phi W}{\rho C_p}\Delta N \quad (2)$$

where

$$\phi \equiv 1 - \frac{\Phi\Delta H}{h\nu}$$

where W is the molecular weight, C_p is the heat capacity, ρ is the density, $h\nu$ is the photon energy of excitation light, ΔN is the number of the reacting molecules in a unit volume, and Φ is the quantum yield of the reaction. We can determine $\Phi\Delta H$ by comparison with the signal intensity of a reference sample under the same experimental conditions. The ratio of the refractive index change for the sample [δn(sample)] to that for reference [δn(ref)] is given by

$$\frac{\delta n_{th}(\text{sample})}{\delta n_{th}(\text{ref})} = 1 - \frac{\Phi\Delta H}{h\nu} \quad (3)$$

Since the TrL signal reflects the refractive index change by the photoexcitation, the information from the signal is essentially identical to that obtained from the TG method. One notable difference is the decay rate constant of the signal. The decay rate of the thermal grating signal under the present experimental conditions is in a range of a few microseconds to 50 μs, whereas that of the thermal lens signal is ~10 ms because the decay rate of this lens signal is determined by the thermal diffusion time across the beam diameter (~100 μs). While the thermal energy released after ~100 μs cannot be detected by the TG method, e.g., the pR → pB process, it can be detected by the TrL method.

Since the TrL signal decays much more slowly than the thermal grating signal and is even comparable to the rate of the back-reaction pB → pG, it is practically impossible to separate the thermal contribution from the other (species lens) contributions by the time-resolved measurement. Here we made a preliminary measurement of the enthalpy change during the pR → pB process by making use of the temperature-dependent dn/dT in eq 2. Because the magnitude of the thermal component (δn_{th}) is proportional to dn/dT, we can measure the contribution of δn_{th} by changing dn/dT, which can be accomplished by changing the temperature. This is the traditional technique to separate the thermal contribution in the PA signal (*1*−*3*). Using the separated δn_{th} value, ΔH can be calculated by eq 3.

RESULTS

ΔH and ΔV of the First Step (pG → pR). Figure 1 depicts the TG signal of the PYP solution after excitation at 465 nm with a repetition rate of 1−0.5 Hz. This repetition rate

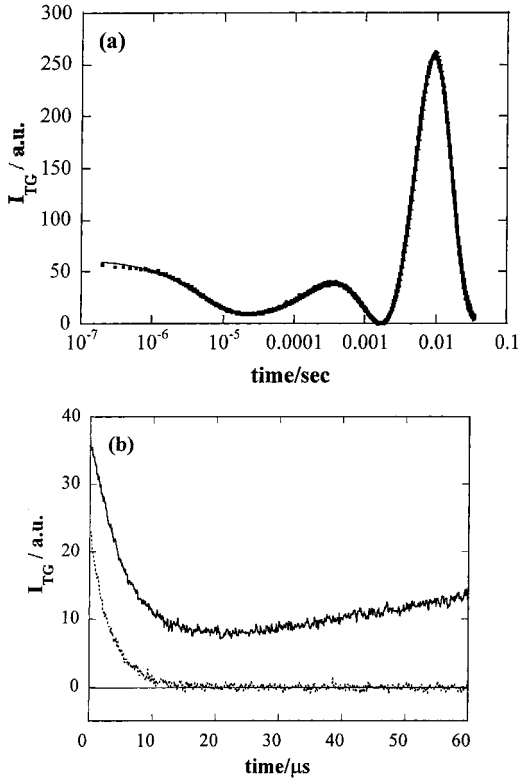

FIGURE 1: (a) Temporal profile of the TG signal of PYP solution (10 mM Tris-HCl buffer) excited at 465 nm (dotted line). The solid line is the best fitted curve using the method described in the text. (b) Comparison between the TG signal of the PYP sample in a short time range (solid line) and the thermal grating signal of BCP (dotted line).

is, in particular at low temperatures, faster than the inverse of the photocycle rate of PYP. However, the final decay rate in the 100 ms range of the TG signal is determined by the molecular diffusion process, which is faster than the intrinsic reaction rate as described later. Therefore, the slowest return rate to pG is not an important kinetics in this measurement. Furthermore, since the pump light (less than 5 μJ/pulse) excites less than 10% of PYP in the illuminated region and the excitation is spatially inhomogeneous for the TG measurement, the photoexcited PYP molecule should be relaxed or diffused away before the next excitation pulse comes in. Hence we can neglect the multiple excitation of PYP at any temperature. We confirmed that decreasing the repetition rate further did not change the observed TG signal within our experimental uncertainty.

The signal rises quickly after the excitation and decays with a lifetime of several microseconds, which depends on the grating wavenumber. At first glance, the TG signal of PYP seemed to rise completely within the excitation pulse (10 ns) as described previously (*26*). However, a careful examination reveals that, after the dominant signal rises within 10 ns, there appears a weak slow rising with about a 1 μs time constant. This slow rise was unexpected because the photoisomerization of the chromophore undergoes very quickly (<2 ps), and the transient absorption signal showed no time dependence of pR after the 3 ns dynamics until the 200 μs kinetics for pR → pB (*32*). Hence, the slower dynamics around the 1 μs time constant is a new dynamics, which has not been reported so far and cannot be detected by the absorption technique. This dynamics may represent

the dynamics of amino acid residues that locate far from the chromophore. We represent this dynamics as $pR_1 \rightarrow pR_2$, and pR is reserved to indicate both pR_1 and pR_2 in this paper. Since this dynamics is clearer for PYP mutants, we will discuss this dynamics in a separate paper including the results of mutants. In the present paper, we will consider the thermodynamic and transport properties of pR_2. After the decay, the signal shows a growth decay feature twice during a few millisecond time scale. Since there is no optical absorption from the original species (pG) and any intermediates of PYP at the prove wavelength (633 nm), the observed TG signal must come from the refractive index change after the photoexcitation. We found that the TG signal in the entire region can be well reproduced by the square of the summation of five exponential functions:

$$I_{TG} = \alpha[A \exp(-k_A t) + B \exp(-k_B t) + C \exp(-k_C t) + D \exp(-k_D t) + E \exp(-k_E t)]^2 \quad (4)$$

where α is a constant, $A-E$ are preexponential factors, and k_A-k_E ($k_A > k_B > k_C > k_D > k_E$) are rate constants. However, unless we fix some parameters among $A-E$ and k_A-k_E, it is almost impossible to determine these parameters uniquely by the curve fitting even in this wide time range. We examined the origins of these components and were able to determine some of the rate constants as follows.

First, the fastest decay rate constant, k_A, can be rather easily determined independently using the "calorimetric reference" sample. BCP has been sometimes used as a calorimetric reference sample, because the photoexcited state of BCP relaxes to the ground state very rapidly without any photochemical reaction. Therefore, the TG signal after the photoexcitation of BCP consists of only the thermal grating component. The TG signal of BCP measured under the same condition as the PYP sample is shown in Figure 1b. Comparing the decay rate of the PYP signal with that of the BCP signal, we attribute the signal of PYP decaying in several microseconds to the thermal grating signal. Hence, we can fix k_A to $D_{th}q^2$, which can be measured independently from the decay of the thermal grating signal of BCP. The intensity of this component represents the thermal energy released by the first step, $pG^* \rightarrow pR_2$. (The amount of the thermal energy is determined by the single-exponential fitting from 1.5 μs after the photoexcitation. Hence ΔH of this species is ΔH of pR_2.)

Second, measuring at different grating wavenumbers (q), we found that the decay of the thermal grating and the kinetics of the second growth decay signal (k_D and k_E) varied depending on q, while the other two rate constants (k_B and k_C) did not depend on q. This dependence is apparent when q was very small (e.g., $q^2 < 1 \times 10^{12}$ m^{-2}). Under this small q condition, the kinetics of k_D and k_E are well separated from the other kinetics of k_A, k_B, and k_C, although the values among the sets of (k_D and k_E) and (k_B and k_C) are not uniquely determined.

The kinetics which does not depend on q should represent the reaction dynamics of PYP. Considering the time scale, this dynamics should be the $pR_2 \rightarrow pB$ process. The kinetics of $pR_2 \rightarrow pB$ can be monitored by the transient absorption technique as reported previously (*17*, *18*). The time profile probed at 476 nm is depicted in Figure 2. Initially, the probe light intensity decreases (enhanced absorption) quickly after excitation within the 10 ns pulse width, then gradually it changes to the bleach signal. This feature is consistent with the previous transient absorption studies of the PYP system (*17*, *18*). The initial enhanced absorption and the subsequent bleach signals were attributed to pR and pB, respectively. The temporal profile associated with the $pR \rightarrow pB$ transformation can be fitted by a biexponential function with lifetimes of 170 μs and 1.0 ms. These lifetimes agree well with those reported before from the global analysis of the absorption change (*19*). Hence we used 170 μs and 1.0 ms for k_B^{-1} and k_C^{-1}.

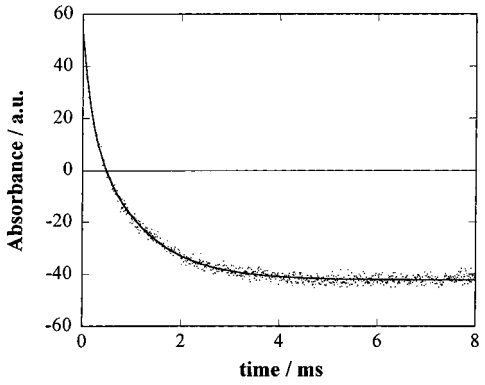

FIGURE 2: Time profile of the transient absorption probed at 476 nm (dotted line) and the best fitted curve by the biexponential function (solid line).

The kinetics that depends on q should be attributed to the molecular diffusion process. Since the chemical species that exist in this time scale are pG and pB, the rate constants k_D and k_E should be equal to $D_{pG}q^2$ and $D_{pB}q^2$. (D_{pG} and D_{pB} are the diffusion coefficients of pG and pB, respectively.) There are two possibilities for the diffusion kinetics: $k_D = D_{pG}q^2$ and $k_E = D_{pB}q^2$ or vice versa. We can identify the diffusing species from the signs of the preexponential factors. The preexponential factor, A, should be proportional to δn_{th} given by eq 2, and the sign of A must be negative (dn/dT at this temperature is negative). To reproduce the observed signal, the signs of B, C, and E should be positive and D must be negative. Here, we should note that the preexponential factor of the species grating signal is determined by the refractive index change due to the presence of the species (*9*). Considering that the wavelength of the probe light is on the red side of the absorption spectra of pB, we can reasonably predict that the refractive index due to the presence of pG and pB should be positive. Therefore, the creation of pB contributes to the positive refractive index. On the other hand, since the phase of the spatial concentration modulation of pG is 180° shifted to that of pB, the sign of the preexponential factor is predicted to be negative. Hence the depletion of pG and creation of pB should induce negative and positive refractive index changes, respectively. According to these considerations, $D < 0$ and $E > 0$, k_D and k_E should correspond to $D_{pG}q^2$ and $D_{pB}q^2$, respectively. The determination of D, E, D_{pG}, and D_{pB} will be described later (see Diffusion Constants of pG and pB).

In summary, the TG signal in the entire time region after photoexcitation of PYP is expressed by the equation:

$$I_{TG} = \alpha[A \exp(-D_{th}q^2 t) + B \exp(-k_B t) + C \exp(-k_C t) + D \exp(-D_{pG}q^2 t) + E \exp(-D_{pB}q^2 t)]^2 \quad (5)$$

Table 1: Preexponential Factors and Lifetimes Determined from the Fitting of the Observed TG Signal at $q^2 = 1.5 \times 10^{12}$ m^{-2}

T/°C	A	k_A^{-1}/μs	B	k_B^{-1}/μs	C	k_C^{-1}/ms	D	k_D^{-1}/ms	E	k_E^{-1}/ms
20.5	−6	4.6	6.5	170	10.5	1.0	−216.5	5.3	197.2	6.9
16.7	−5.2	4.6	4.9	200	16.0	1.3	−210.0	6.0	187.3	8.1
12.4	−3.6	4.6	3.7	250	16.3	1.6	−203.4	7.3	181.2	9.7
8.4	−1.6	4.6	4.7	300	15.0	1.8	−209.9	8.5	180.5	11.2

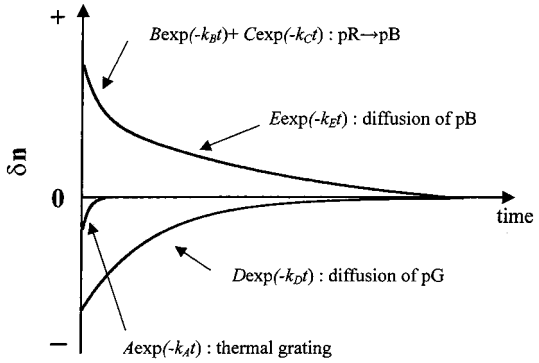

FIGURE 3: The origin of the observed TG signal in Figure 1 is decomposed into several components and schematically illustrated.

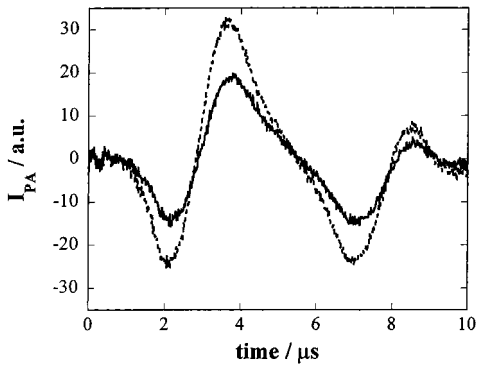

FIGURE 4: PA signals of the PYP solution (solid line) and the reference sample (dotted line) under the same experimental condition at 21 °C.

Here, the first term on the right-hand side represents the thermal grating component due to the decay from the excited state of pG (pG*), the second and third terms are the kinetics of the $pR_2 \rightarrow pB$ transformation, and the fourth and fifth terms represent the diffusion of pG and pB. The temporal profiles of the refractive index change of these terms are illustrated in Figure 3. From the fitting of the observed TG signal by eq 5 in the entire time region at various temperatures, we can determine a variety of properties of pG as well as the intermediate species. The parameters (amplitudes and lifetimes) obtained from the least-squares fitting of the TG signal at several temperatures are listed in Table 1.

An advantage of this TG measurement is that we can quantitatively separate the energetic contribution (δn_{th}) in the signal without any assumption. This advantage becomes obvious if we compare it with the PA method. Using the PA technique, the thermal and volume contributions cannot be separated unless the sample temperature is changed, and the PA signal intensities at various temperatures are plotted against the thermal expansion coefficient of the solution (*1*−*3*). If ΔH and/or ΔV depend on temperature, the value from this method cannot be correct. Now the TG method can provide ΔH and ΔV without any assumption and also provides an opportunity to investigate the temperature dependence of ΔH and ΔV. For the sake of further discussion, we here shortly summarize ΔH, ΔV, and the temperature dependence of ΔV of PYP (*26*).

The thermal grating signal, $A \exp(-k_A t)$ term, represents the released energy from the photoexcited PYP. Comparing the thermal grating signal intensity with that of BCP, we can determine the stored energy in pR_2, i.e., the enthalpy change for $pG \rightarrow pR_2$ (ΔH_1). From eq 3, we obtain $\Phi \Delta H_1 = 57 \pm 7$ kJ/mol. Using the quantum yield of the reaction $\Phi = 0.35$ (*33*), ΔH_1 is determined to be 160 ± 20 kJ/mol. Two different quantum yields of the reaction were reported independently [$\Phi = 0.64$ by Meyer et al. (*18*) and Devanathan et al. (*32*); $\Phi = 0.35$ by Van Brederode et al. (*33*)]. If we use $\Phi = 0.64$, ΔH_1 should be 90 ± 10 kJ/mol. In this paper, we use $\Phi = 0.35$, because it was measured under a weak excitation laser power condition as we did and also because we can compare our ΔH and ΔV with their reported ones using the same Φ. ΔH and ΔV by using $\Phi = 0.64$ can be easily calculated from the values reported in this paper. The choice of these Φ does not change our discussion and conclusion.

At the same time, from the PA signal (Figure 4) and ΔH_1 determined from the TG measurement, we calculated $\Phi \Delta V$ associated with the $pG \rightarrow pR_2$ transformation. Using $\Phi = 0.35$, the volume contraction of $\Delta V = -7 \pm 2$ cm^3/mol was obtained at 20 °C (*26*). The relative quantum yield of the reaction was monitored by the amplitude of the initial rise of the transient absorption signal (Figure 2) at various temperatures (*26*). We analyzed TG and PA signals at various temperatures, taking this temperature-dependent Φ into account. As a result, we found that the absolute volume contraction indeed increases with decreasing temperature. At 0 °C the volume change becomes ~ -15 cm^3/mol, which is about twice as large as that at room temperature. We will discuss this temperature-dependent ΔV later.

ΔH of the Second Step ($pR_2 \rightarrow pB$). Since the decay of the thermal grating signal is generally much faster than the kinetics of $pR_2 \rightarrow pB$, the TG signal due to the thermal energy released by this process is too small to be determined. For studying the enthalpy of the pB state (ΔH_2), we used the TrL method. The decay of the TrL signal is on an order of tens of milliseconds, and the thermal energy released by the $pR_2 \rightarrow pB$ process can be detected clearly as the rise of the signal.

Figure 5 shows the TrL signals of PYP and the reference sample. The TrL signal of PYP initially rises very fast (with the response time of the thermal lens signal) and then slowly. This TrL signal was fitted by a fast rise with an instrumental response time constant and a single-exponential function. The first rise corresponds to the transformation $pG \rightarrow pR_2$. The slower rise rate (e.g., 340, 410, 550, and 630 μs at 20, 16.6, 8.8, and 4.8 °C, respectively) should be attributed to the transformation $pR_2 \rightarrow pB$. The reason this $pR_2 \rightarrow pB$ process is not biexponential as observed by the TG and TA signals is not clear at present. However, for the purpose here, we

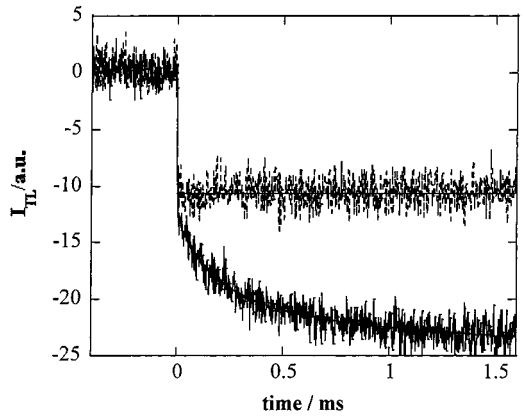

FIGURE 5: TrL signals of the PYP solution (solid line) and the reference sample (dotted line) at 21 °C. The smooth solid lines are the best fitted curves (see text).

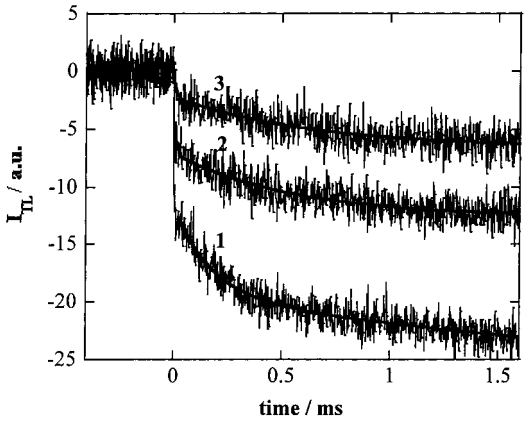

FIGURE 6: TrL signals of the PYP solution at various temperatures (1, 20.5 °C; 2, 8.8 °C; 3, 1.2 °C). The smooth solid lines are the best fitted curves (see text).

need only the signal intensity, and the difference in the time profile between the TG and TrL signals will be investigated in the future.

The TrL signal intensity of PYP is much larger than that of the reference sample, because δn_{spe} is constructively overlapped with δn_{th} of PYP (both δn_{spe} and δn_{th} possess negative signs). The sign of δn_{spe} is consistent with the result from the TG measurement. Contrary to the TG experiment, it is not trivial to separate the thermal contribution from the species lens signal in the TrL case because the decay of the thermal lens signal is so slow that the magnitude of the thermal component alone cannot be separated. Hence, here we used the traditional technique to separate the thermal intensity from the other contributions: the temperature dependence method. As we have mentioned in the previous section, this method, assuming temperature-independent ΔV for $pR_2 \rightarrow pB$, may lead to an inaccurate ΔH. However, this method may provide an estimation of ΔH_2 and will be used until more a accurate value is obtained.

The temperature dependence of the TrL signal (Figure 6) shows that both of the fast and slow rise components become weaker and the slower rise rate becomes slower with decreasing temperature. The magnitudes of the fast rise component (δn_1) and the slow rise component (δn_2) of the TrL signal are plotted against dn/dT in Figure 7. Because the contribution from δn_{th} disappears at the temperature of

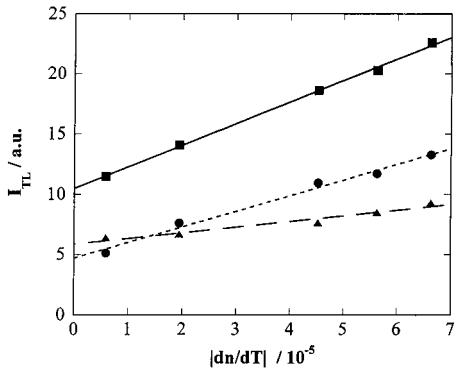

FIGURE 7: Plots of the intensity of the first rising component (circles) and the slow rising component (triangles) and total intensity (squares) of the TrL signal versus $\delta n/\delta T$ and the linear fittings.

Table 2: Separation of the Fast (δn_1) and Slow (δn_2) Rising TrL Signal into the Thermal Lens (δn_{th}) and Species Lens (δn_{spe}) Components Using the Temperature Variation Method[a]

	δn_{th}	δn_{spe}
$pG^* \rightarrow pR_2$ (δn_1)	0.74	0.55
$pR_2 \rightarrow pB$ (δn_2)	0.18	0.68
total	0.92	1.23

[a] See Figure 7. The intensity of these components is normalized by the thermal lens intensity of the reference sample.

$dn/dT = 0$, the TrL signal intensity at this temperature corresponds directly to the magnitude of δn_{spe}.

From this signal intensity, we can separate δn_{th} from δn_{spe}. After considering the temperature dependence of Φ, we calculate the relative δn_{th1}, δn_{th2} (the thermal lens contributions of the fast and slow rising components to total δn, respectively), δn_{spe1}, and δn_{spe2} (the species lens contributions of the fast and slow rising components, respectively). The result is shown in Table 2. For the $pG \rightarrow pR_2$ step (δn_{spe1}), the data from the TrL signal is consistent with the result from the TG measurement. By comparing δn_{th2} with δn_{th} of the calorimetric reference sample, we determine the enthalpy difference between pG and pB (ΔH_2). Again using $\Phi = 0.35$, we obtain $\Delta H_2 = 60 \pm 30$ kJ/mol. Although we have to examine the temperature dependence of ΔV for $pR_2 \rightarrow pB$ before making a definitive conclusion, ΔH_2 should not be so much different from this value unless the temperature dependence of the volume change is extremely large.

Diffusion Constants of pG and pB. One of the unique advantages of the TG detection is that the diffusion coefficients (D) of transient species can be measured. In the observed TG signal (Figure 1), the latest grow decay part represents the diffusion process. This part should be fitted by a biexponential function of the fourth and fifth terms of eq 5. However, as sometimes pointed out (*34*), when the two rate constants are close each other, a reliable biexponential fitting is not simple. With four parameters, in this case D, E, D_{pG}, and D_{pB}, the least-squares fitting converges with several different parameters depending on the initial values. To reduce the ambiguity, we must make some restrictions for the fitting parameters. For that purpose, we use the information from the TrL signal. In principle, the origin of the TG signal should be the same as that of the TrL signal. Therefore, the TG signal intensity for the molecular diffusion signal, $D + E$, should correspond to $\delta n_{spe1} + \delta n_{spe2}$ in the TrL case. While the four-parameter

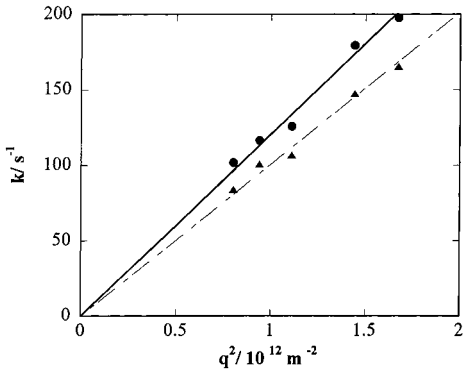

FIGURE 8: q^2 plots of the decay rate constant (k) of the two diffusion components in the TG signal and the least-squares fits (circles and solid line for pG; triangles and dotted line for pB).

fitting (D, E, D_{pG}, D_{pB}) is required for the TG case, the TrL signal intensity of ($\delta n_{spe1} + \delta n_{spe2}$) is much easier to be determined because the decay rate of ($\delta n_{spe1} + \delta n_{spe2}$) is almost negligible in this time range. Hence we can fix $D + E$ using ($\delta n_{spe1} + \delta n_{spe2}$) determined from the TrL measurement. Under this restriction, we fit the TG signal by the least-squares method. The time constants of two exponential functions ($D_{pG}q^2$, $D_{pB}q^2$) are plotted against q^2 (Figure 8). From the slope of the least-squares fit of these plots, we can obtain D of pG and pB as 1.21×10^{-10} and 1.00×10^{-10} m^2/s, respectively.

Diffusion of Denatured PYP. For the interpretation of the smaller D of pB compared with that of pG, we measured D of various unfolded conformations of PYP using a denaturant. Very recently, Ohishi et al. used urea as the denaturant to study the light-induced stabilization (*27*b). Here we used guanidine hydrochloride (GdnHCl), because GdnHCl is known to be a more efficient denaturant for many proteins and the protein structure can be unfolded with a smaller amount of the denaturant, which is important not to change the solution properties (e.g., viscosity) significantly. For example, the viscosity of a 4 M GdnHCl solution is not so much different from that of water compared with a 6 M urea solution (*35*). First, the influence of GdnHCl on PYP stability was investigated by the absorption spectra and CD ellipticity of PYP. With increasing GdnHCl concentration at pH = 7.0, the contribution of the absorption band peaked at 446 nm decreases and that of the absorption band at 339 nm increases. This change can be explained in terms of the movement of the chromophore from the hydrophobic core of the protein interior to solvent. CD ellipticity at 223 nm also decreases with increasing the GdnHCl concentration. This decrease indicates the destruction of the secondary structure of PYP protein by GdnHCl. These changes are very similar to those observed by adding urea as the denaturant previously. Data on the equilibrium GdnHCl-induced unfolding of PYP at pH = 7.0 monitored by the absorbance at 446 nm and CD intensity at 223 nm are presented in Figure 9. Both cases show a cooperative unfolding transition on addition of denaturant. The obtained values are fitted by assuming a two-state model with an equilibrium between the native and denatured states (Figure 9). The C_m value, which is the transition midpoint concentration of GdnHCl for unfolding the protein, is frequently used as a probe for the protein stability (*36*). It is 2.4 and 2.7 M from the absorbance and CD ellipticity detected at 223 nm, respectively. These values are much smaller than those obtained by the urea concentration measurements (*27*b).

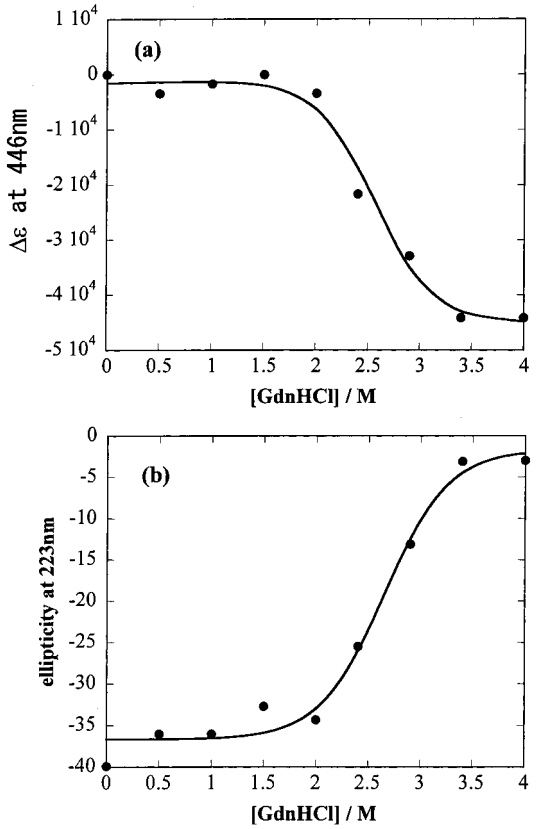

FIGURE 9: GdnHCl unfolding transition of PYP monitored by the absorbance at 446 nm (a) and CD ellipticity at 223 nm (b) vs GdnHCl concentration. The solid lines are the results of nonlinear least-squares best fits by the two-state model.

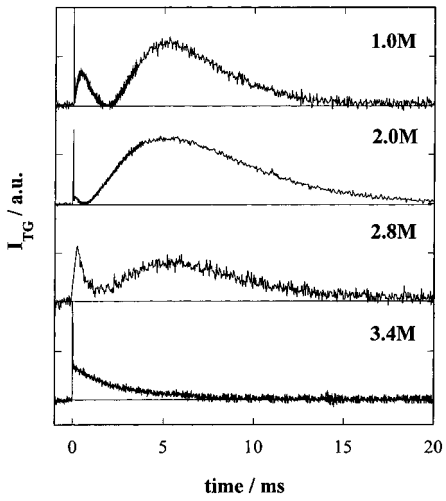

FIGURE 10: TG signals of PYP in 1.0, 2.0, 2.8, and 3.4 M GdnHCl solution.

When PYP is denatured, PYP does not undergo the normal photocycle reaction even by photoirradiation. However, we observed a population grating signal after the photoexcitation of even sufficiently denatured PYP ([GdnHCl] = 4 M). For example, Figure 10 depicts the TG signals of PYP in 1.0, 2.0, 2.8, and 3.4 M GdnHCl solutions. Since only a photochemical reaction can give rise to the population grating through the change of the refractive index, the appearance of the population grating indicates that, even if PYP is

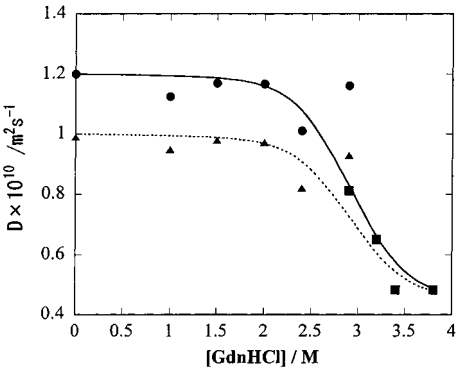

FIGURE 11: Diffusion coefficient of each state (pG, circles; pB, triangles; denatured, squares) of PYP at various GdnHCl concentrations. The viscosity change by addition of GdnHCl was corrected by a method described in the text.

denatured, the trans to cis photoisomerization of the chromophore takes place. This reaction is conceivable because we previously observed the population grating signal of *p*-coumaric acid in water after photoexcitation (*37*). Hence the protein is not necessary for the isomerization reaction. On the other hand, the back-isomerization, cis to trans, is different. We noticed that the grating signal intensity becomes weaker with successive pulse irradiations. This weakening can be explained by a much slower or no back-isomerization for the denatured PYP than that for the native PYP. This fact suggests that the protein environment enhances the back-isomerization compared with water solvent. This catalytic action of the protein to back-isomerization was previously suggested by the thermodynamic measurement of the activation enthalpy of pB → pG (*38*). Because of this slow back-reaction, we do not need to consider the back-reaction as the source of the decay of the grating signal, and the grating decay solely comes from the diffusion process of the denatured PYP.

The population grating signal under the fully denatured PYP condition can be fitted well by a single-exponential function. The decay rate constant is given by Dq^2. In this case, D of PYP with the trans form of the chromophore should be the same as that with the cis form. This is sharply in contrast to the native PYP, in which D of pG is different from that of pB. Again this difference can be explained by the denatured conformation of PYP; that is, the chromophore is present in the water phase rather than in the protein interior, so that the trans to cis isomerization does not influence the diffusion process. This is consistent with the previous observation that the D of the trans form and cis form of *p*-coumaric acid are very similar (*36*). This fact also supports that the difference in D between pG and pB comes from the different protein structure.

From the decay rate of the TG signal, D was calculated at various GdnHCl concentrations. However, the change in D reflects not only the decrease of D of PYP due to the structural change but also the change in the viscosity simply by the addition of GdnHCl to the solvent. For the correction of this viscosity change, we normalize D by multiplying η_0/η [η_0, the viscosity of the buffer; η, the viscosity of the GdnHCl solution (*35*)]. D of PYP at various GdnHCl concentrations is shown in Figure 11.

The double-exponential feature represents the native form of PYP, whereas the single-exponential feature indicates the denatured PYP. It is interesting to note that the double-exponential and single-exponential components exist simultaneously at 2.8 M GdnHCl (Figure 10) instead of a gradual change from the double-exponential form to the single-exponential form. This coexistence of the native and denatured PYP in this time range implies that the protein transformation between the native and denatured conformations is slower than ~10 ms time scale.

DISCUSSION

Enthalpy Changes. Our result on ΔH ($\Delta H_1 = 160$ kJ/mol, $\Delta H_2 = 60$ kJ/mol) clearly indicates that the energy of the pR_2 state is astonishingly high, and during the $pR_2 \rightarrow$ pB process, large energetic stabilization takes place. (Again, we have to notice that ΔH_2 was determined by assuming the temperature independence of ΔV for the $pR_2 \rightarrow$ pB step, which may not be correct as the activation entropy and activation heat capacity for this step depend on temperature (*38*). However, this ΔH_2 value may not be so much different for the present qualitative discussion even if we take this effect into consideration.) A time-resolved X-ray study (*22*) showed that the trans to cis isomerization is completed in less than 1 ns. From the energetic point of view, these facts suggest that the protein part has not relaxed yet to adopt a new conformation of the chromophore; that is, the protein structure is strained in pR_2. This strain may cause the large enthalpy of the pR_2 species. It is reasonable to speculate that the following step ($pR_2 \rightarrow$ pB) is driven by this stored energy in pR_2. In pB, the whole protein structure is relaxed to adopt to the cis form of the chromophore, and this relaxation causes the lower enthalpy of pB. This feature is similar to the case of a typical visual signal transducer, the rhodopsin (*39*, *40*). In this protein, the enthalpy is very high up to the batho intermediate (130 kJ/mol) and suddenly decreases to 50 kJ/mol in the next step (*39*). From the energetic point of view, the pR_2 state of PYP is similar to the batho of rhodopsin.

It is interesting to note that the enthalpy difference between the trans and cis isomers of *p*-coumaric acid in water is about 50 kJ/mol. From this fact, the enthalpy of pB seems to come from only the unstable energy of the cis chromophore, but we should note that the coumaric acid in pG is deprotonated and this chemical change should be taken into account. We may compare ΔH_2 with that previously obtained ΔH for the chemically created pB-like state (pB_{dark}). PYP is known to be very stable against the thermal denaturation, but it can be reversibly denatured by decreasing the pH below 3.25 (*13*, *38*). Using the denaturing (heat) treatments at this low pH, a form of the protein absorbing near 345 nm (pB_{dark}) can be reversibly created from pG. Van Brederode et al. have measured ΔH between pG and pB_{dark} using the standard calorimetric method and reported it as 52.1 kJ/mol. It is surprising that spectroscopically obtained ΔH_2 for photo-created pB is very similar to that of denatured pB_{dark}, because the photochemically created pB possesses the cis chromophore, while the chemically created denatured pB_{dark} should have the trans chromophore. Ohishi et al. measured the free energy change upon denaturation for pG and pB at low pH (pH = 5). The difference in the free energy of the protein part between pG and pB was estimated to be about 15 kJ/mol, which is much smaller than the enthalpy change

of the chromophore (about 50 kJ/mol). Hence our result here is consistent with their result to suggest almost completely relaxed protein structure in pB.

Volume Change. In recent years, a number of investigators have applied many perturbations (e.g., temperature, denaturant, pH, pressure) to reversible folding proteins and studied the characteristic features of unfolded proteins. The partial molar volume of a protein is a macroscopic observable which is particularly sensitive to the hydration properties of solvent-exposed atomic groups as well as to the structure, dynamics, and conformational properties of the solvent. Here we determined that the volume change by pG → pR_2 is negative (−7 mL/mol at 20 °C).

The partial molar volume of a solute can be described as a sum of the following basic contributions (*15*): (1) constitutive volume, which is the sum of the van der Waals volumes of all of the protein constitutive atoms; (2) void volume, the volume of the structural voids within the solvent-inaccessible core of the protein that result from imperfect atomic packing (V_V); (3) thermal motion contribution, a space required for heat motion at nonzero temperature; (4) interaction volume, the effects of solute−solvent interactions caused by electrostriction around charged groups or by the hydrogen bonding of polar groups with water; (5) translational thermal motions of molecules ($\kappa_T k_B T$: κ_T, isothermal compressibility). Usually this is negligible in large molecules such as protein.

The van der Waals volume is conserved during the reaction; hence it does not contribute to the volume change here. It is interesting to note that the molecular volume change of a size of PYP is usually (slightly) negative by the native to unfolding process (*41*). This contraction of the protein volume by the unfolding process has been explained in terms of multiple contributions from the above factors as follows. The solvation of polar groups and charged groups causes a decrease in volume. In addition, the transfer of nonpolar groups from hydrophobic to aqueous environments upon protein denaturation also causes a decrease in volume since the volume changes due to hydration are negative. The change in the void volume due to imperfect protein packing is also expected to be negative upon denaturation. On the other hand, "thermal volume", which results from thermally induced molecular vibrations of both the solute and solvent molecules, thereby leads to an expansion of the solvent. These contributions cancel each other, and as a result, the volume change upon unfolding for "small" proteins is predicted to be small negative. The observed small volume contraction by the pR_2 formation is consistent with this prediction, so that we may speculate that the pR_2 formation process can be considered as the denaturation process of the protein part. On the basis of this interpretation, the negative volume change may suggest that the solvent-accessible surface areas increase by the pG → pR_2 process, because the average hydration contribution to the protein partial volume is proportional to the solvent-accessible surface areas of the protein; $\Delta V_h \propto S_A$. This is consistent with the other observations in the present study as shown in the later sections.

From the measurement of the heat capacity of pB_{dark}, it was suggested that this form is, not totally but at least partially, unfolded random coil conformation (*38*). Furthermore, comparing the activation heat capacity $\Delta C_p^{\ddagger}$ associated with the PYP photocycle with the other proteins, the pR → pB transition was suggested to be thermodynamically equivalent to a protein unfolding reaction (*38*). Apparently the features of the transition states $pR^{\ddagger}$ and $pB^{\ddagger}$ in the PYP photocycle are similar to those of the transition states for the (un)folding of small globular water-soluble proteins. We showed, in this study, that not only from the activation heat capacity or the heat capacity of the chemically created pB_{dark} state but also from the partial molar volume change of pR_2, the pR_2 state may be interpreted as the unfolded protein structure. It may be interesting to compare ΔV with the volume change by the complete unfolding process. Although there are no data available for PYP so far, we may use a calculated value from an equation proposed before (*41*). It was found that the specific partial molar volume has a correlation with the molecular weight. According to this empirical equation, $\Delta V = -950$ mL/mol is predicted for the complete unfolding of PYP. Compared with this value, the observed ΔV for pG → pR_2 is much smaller (less than 1%). This is reasonable because pR_2 cannot have a fully denatured structure. A recent time-resolved FT-IR experiment indicated that a significant change in the amide I band was not observed, which suggests that the protein does not fully respond to chromophore isomerization (*25*). This is consistent with our observation here. In the following sections, we further examine the (partially) denatured structures of the reaction intermediate pR_2 and pB in view of various aspects.

Temperature Dependence of ΔV. The partial molar volume changes in irreversible reactions in water have been measured mainly by the laser-induced PA method with an assumption that ΔV does not depend on temperature. Since there was no alternative way, this assumption has never been tested rigorously. Using the time-resolved TG and PA hybrid method, we could detect a rather large temperature-dependent ΔV for the first time (*26*). Previously, we interpreted this temperature- dependent ΔV_1 in terms of many possible local minima of the potential curve along the reaction coordinate (*26*). Here we consider this phenomenon from a different perspective.

The slope of the plot, ΔV vs T, corresponds to $\Delta\alpha_{th}$ [$\Delta\alpha_{th} = (\partial V/\partial T)_p$], which is the change in the coefficient of thermal expansion for the initial (pG) and the intermediate (pR_2) forms. This indicates that the thermal expansivity of pR_2 is larger than that of pG. This is an interesting observation, not only because this is the first example to show the different α_{th} between the reactant and the reaction intermediate but also because previous studies on the thermodynamic properties of proteins have already clearly showed that the partial molar volume of the unfolded state increases more significantly with temperature than that of the folded state (*42*). Hence this observation, temperature-dependent ΔV, also indicates the resemblance of the pR_2 state to the unfolded state of the protein. The larger α_{th} for unfolded protein is intuitively understandable if one considers that the unfolded protein has a loose protein structure, which is expected to be more sensitive to the temperature. In fact, α_{th} is proportional to the cross-correlation of the volume (V) and entropy (S) fluctuations (*43*, *44*)

$$\langle SV - \langle S\rangle\langle V\rangle\rangle = kTV\alpha_{th} \qquad (6)$$

where $\langle\ \rangle$ indicates the ensemble average and k is the Boltzmann factor. The larger α_{th} is an indication of larger

structural and/or entropy fluctuation. Therefore, even in this initial intermediate species pR_2, which is created after 1 μs of photoisomerization of the chromophore, the protein structure is loosened. Apparently, the structural change is not restricted around the chromophore, which is contrary to the results from the time-resolved X-ray experiment (*22*). The difference of α_{th} between the folded and unfolded metmyoglobin (metMb) was reported to be $\Delta\alpha_{th} = +2.4$ mL/(mol·K) (*45*), while $\Delta\alpha_{th}$ for pG and pR_2 of PYP was +0.6 mL/(mol·K). If we tentatively assume that $\Delta\alpha_{th}$ for metMb is a typical value for $\Delta\alpha_{th}$ of the native and unfolded conformation, the fluctuation of pR_2 is about 25% unfolded from pG. This value cannot be considered too seriously, but we believe that this is a right order of magnitude of the partially loosed structure.

A recent time-resolved FT-IR experiment does not show a large backbone amide group movement in pR (*25*). Furthermore, ΔV described in the previous section from the TG measurement is much smaller than expected from the unfolding process. These results (TG and FT-IR) suggest that the conformation of pR is not changed significantly from pG. Therefore, the larger thermal expansivity in pR_2 indicates that the rigidity of the structure is weakened with a small conformational change. Apparently, this weakening is caused by the strain induced by the photoisomerization of the chromophore as suggested from the large enthalpy of this species. This larger conformational flexibility in pR_2 may cause the next larger protein structural change in $pR_2 \rightarrow$ pB.

Diffusion Coefficient. In the characterization of native and non-native states of proteins in solution, a measurement of the molecular dimensions of the system is valuable. A measure of the average dimensions of the conformational ensemble can give information about the nature of the structures adopted by the polypeptide chain. *D* can probe the average dimension and the coupling of the local and global conformational properties of these unfolded and partly folded species.

The observed 1.2 times difference between D_{pG} and D_{pB} is a large difference, and in fact it is rather astonishing. In the framework of the Stokes−Einstein theory, *D* is proportional to $kT/\eta r$, where *k* is the Boltzmann constant, *T* is the absolute temperature, η is the viscosity of the solvent, and *r* is the radius of the solute. If the different *D* is due to the volume change from pG to pB, the volume of pB must be $1.2^3 \sim 1.7$ times as large as the volume of pG. If such a large volume expansion occurs, an extremely large δn_v component should be observed. Judging from the profile of the TG signal, this is not the case. Therefore, we presume that this difference of the diffusion coefficient comes from the large change of the interaction between the protein and water molecules in pG and pB. According to the time-resolved crystallography, the guanidinium group of Arg 52 moves toward solvent in the pB state, and the phenolic oxygen of the head part of the chromophore moves largely from the protein core. As a result, the phenolic oxygen is solvent-exposed and protonated. This change will increase the protein−water interaction, which could be a cause of the slower diffusion constant of the pB species. However, as long as the change is localized around the chromophore, *D* may not be changed so much. We suppose that the surface of the whole protein dramatically changes to hydrophilic character by the transformation from pG to pB.

D cannot represent the real radius of the diffusing species, but this "hydrodynamic radius" gives us an intuitive sense on the radius and the interaction. We consider *D* of PYP from two different approaches below.

One method to connect the intermediate species with the unfolded structure is to use the compact factor *C* introduced by Wilkins et al. (*46*), which is

$$C = (r_h^D - r_h)/(r_h^D - r_h^N) \quad (7)$$

where r_h^D and r_h^N are the hydrodynamic radii for the native and fully denatured states, respectively, and r_h is the experimentally determined hydrodynamic radius. According to this definition the protein with the same molecular radius as the native state will have $C = 1.0$ and that with the same radius as a fully denatured state, $C = 0$. With a slight modification based on the Stokes−Einstein relationship, *C* can be equivalently defined as

$$C = (1/D^D - 1/D)/(1/D^D - 1/D^N) \quad (8)$$

where the superscripts of *D* have the same meaning as above. From this equation, we can say that the pB state possesses about 14% unfolded structure compared with pG.

The other argument is related with the surface corrugation and roughness of globular proteins. Choi et al. recently showed that the magnitude of structural fluctuation and the coefficient of self-diffusion vary with the size of solvent molecules and correlate nicely with the correlation dimension of the protein by using molecular dynamics simulations (*47*). Correlation dimension D_2 is a parameter describing the surface roughness of globular protein molecules, which depends on the size of a guest molecule approaching them. The larger D_2 is, the smaller the diffusion coefficient is. On the basis of this consideration, the smaller *D* of pB means that the surface becomes rougher in pB than pG. This surface roughness should be related with the loosened structure of the pB state as suggested in the above sections.

From a denaturation experiment, Ohishi et al. have suggested that the surface area of pB becomes larger than that of pG (*27*b). Our result here is consistent with their interpretation. Recently, the conformational change from pG to pB was studied by the NMR technique in the solution phase. From the protection factor, it indicates that hydrogen bonding between several residues is significantly weakened in pB compared with pG even at residues far from the chromophore. Breaking the intraprotein hydrogen bonding means that the protein structure becomes rough (larger D_2) and the protein−matrix hydrogen bonding becomes stronger. These two effects make the translational diffusion slower in pB compared with pG. Unfortunately, the correlation between the structural change and the change in *D* has not been well established. Combining the data from NMR and our *D* measurement, we could study how much structural change is necessary to change *D* by 20% in the future.

SUMMARY

We have determined some thermodynamic properties (enthalpy change, volume change) and transport property (diffusion coefficient) of unstable intermediate species of PYP in the time domain by using the pulsed laser-induced

photoacoustic and transient grating method. The enthalpy change indicates that the first intermediate pR_2 form is very unstable (160 ± 20 kJ/mol). Only 33% energy is released as heat from the excited state of PYP (energy of pG* = 240 kJ/mol). Since the enthalpy difference between the cis and trans forms of *p*-coumaric acid in water was estimated to be 50 kJ/mol and the enthalpy of pB was estimated to be 60 kJ/mol, most of the energy is stored as the strain of the protein and/or the strained structure of the chromophore in pR_2. The diffusion coefficient of pB is 20% smaller than that of pG. These observations can be consistently interpreted in terms of the unfolded nature of the protein structure of PYP after photoisomerization of the chromophore. A relatively large temperature dependence of the volume change for pG → pR_2 [+0.6 mL/(mol·K)] indicates a large structural fluctuation in pR_2. This softness of the structure should result from the strain induced by the isomerization of the chromophore and causes a larger structural change in the next step (pR_2 → pB) indicated by the FT-IR measurements (*25*). From *D* of pB, the compact factor of pB is estimated to be 86%, and the surface in the pB state is shown to be rougher than that in the pG state. This is the first observation of the smaller *D* of reaction intermediate proteins. These results indicate that a large protein conformational change must occur in the PYP photocycle and it could be related with the mechanism of signal transmitting of this photoreceptor protein.

REFERENCES

1. Callis, J. B., Parson, W. W., and Gouterman, M. (1972) *Biochim. Biophys. Acta 267*, 348−362.
2. Herman, M. S., and Goodman, J. L. (1989) *J. Am. Chem. Soc. 111*, 1849−1854.
3. Braslavsky, S. E., and Heibel, G. E. (1992) *Chem. Rev. 92*, 1381−1410.
4. (a) Westrick, J. A., Goodman, J. L., and Peters, K. S. (1987) *Biochemistry 26*, 8313−8318; (b) Losi, A., Wegener, A. A., Engelhard, M., and Braslavsky, S. E. (2001) *J. Am. Chem. Soc. 123*, 1766−1767; (c) Losi, A., Wegener, A. A., Engelhard, M., and Braslavsky, S. E. (2001) *Photochem. Photobiol. 74*, 495−503.
5. Strassburger, J. M., Grtner, W., and Braslavsky, S. E. (1997) *Biophys. J. 72*, 2294−2303.
6. Gensch, T., Viappiani, C., and Braslavsky, S. E. (1999) *J. Am. Chem. Soc. 121*, 10573−10582.
7. Terazima, M., Hara, T., and Hirota, N. (1995) *Chem. Phys. Lett. 246*, 577−582.
8. Hara, T., Terazima, M., and Hirota, N. (1996) *J. Phys. Chem. 100*, 10194−10200.
9. Terazima, M., and Hirota, N. (1993) *J. Chem. Phys. 98*, 6257−6262.
10. Terazima, M., Okamoto, K., and Hirota, N. (1995) *J. Chem. Phys. 102*, 2506−2515.
11. Okamoto, K., Terazima, M., and Hirota, N. (1995) *J. Chem. Phys. 103*, 10445−10452.
12. Okamoto, K., Terazima, M., and Hirota, N. (1997) *J. Phys. Chem. A 101*, 5269−5277.
13. Meyer, T. E. (1985) *Biochim. Biophys. Acta 806*, 175−183.
14. Sprenger, W. W., Hoff, W. D., Armitage, J. P., and Hellingwerf, K. J. (1993) *J. Bacteriol. 175*, 3096−3104.
15. Borgstohl, G. E. O., Williams, D. R., and Getzoff, E. D. (1995) *Biochemistry 34*, 6278−6287.
16. Baca, M., Borgstahl, G. E. O., Boissinot, M., Burke, P. M., Williams, D. R., Slater, K. A., and Getzoff, E. D. (1994) *Biochemistry 33*, 14369−14377.
17. Hoff, W. D., Düx, P., Hård, K., Devreese, B., Nugteren-Roodzant, I. M., Crielaard, W., Boelens, R., Kaptein, R., Van Beeumen, J., and Hellingwerf, K. J. (1994) *Biochemistry 33*, 13959−13962.
18. Meyer T. E., Tollin, G., Hazzard, J. H., and Cusanovich, M. A. (1989) *Biophys. J. 56*, 559−564.
19. Hoff, W. D., Van Stokkum, I. H. M., Van Ramesdonk, H. J., Van Brederode, M. E., Brouwer, A. M., Fitch, J. C., Meyer, T. E., Van Grondelle, R., and Hellingwerf, K. J. (1994) *Biophys. J. 67*, 1691−1705.
20. Imamoto, Y., Kataoka M., and Tokunaga, F. (1996) *Biochemistry 35*, 14047−14053.
21. Genick, U. K., Borgstahl, G. E. O., Ng, K., Ren, Z., Pradervand, C., Burke, P. M., Šrajer, V., Teng, T., Schildkamp, W., McRee, D. E., Moffat, K., and Getzoff, E. D. (1997) *Science 275*, 1471−1475.
22. Perman, B., Šrajer, V., Ren, Z., Teng, T., Pradervand, C., Ursby, T., Bourgeois, D., Schotte, F., Wulff, M., Kort, R., Hellingwerf, K. J., and Moffat, K. (1998) *Science 279*, 1946−1950.
23. (a) Düx, P., Rubinstenn, G., Vuister, G. W., Boelens, R., Mulder, F. A. A., Hård, K., Hoff, W. D., Kroon, A. R., Crielaard, W., Hellingwerf, K. J., and Kaptein, R. (1998) *Biochemistry 37*, 12689−12699; (b) Rubinstenn, G., Vuister, G. W., Mulder, F. A. A., Düx, P., Boelens, R., Hellingwerf, K. J., and Kaptein, R. (1998) *Nat. Struct. Biol. 5*, 568−570; (c) Craven, C. J., Derix, N. M., Hendriks, J., Boelens, R., Hellingwerf, K. J., and Kaptein, R. (2000) *Biochemistry 39*, 14392−14399.
24. Kandori, H., Iwata, T., Hendriks, J., Maeda, A., and Hellingwerf, K. J. (2000) *Biochemistry 39*, 7902−7909.
25. (a) Brudler, R., Rammelsberg, R., Woo, T. T., Getzoff, E. D., and Gerwert, K. (2001) *Nat. Struct. Biol. 8*, 265−270; (b) Xie, A., Kelemen, L., Hendriks, J., White, B. J., Hellingwerf, K. J., and Hoff, W. D. (2001) *Biochemistry 40*, 1510−1517.
26. Takeshita, K., Hirota, N., Imamoto Y., Kataoka, M., Tokunaga, F., and Terazima, M. (2000) *J. Am. Chem. Soc. 122*, 8524−8528.
27. (a) Imamoto, Y., Ito, T., Kataoka, M., and Tokunaga, F. (1995) *FEBS Lett. 374*, 157−160; (b) Ohishi, S., Shimizu, N., Mihara, K., Imamoto, Y., and Kataoka, M. (2001) *Biochemistry 40*, 2854−2859.
28. Terazima, M., and Hirota, N. (1992) *J. Phys. Chem. 96*, 7147−7150.
29. Terazima, M., Hara, T., and Hirota, N. (1993) *J. Phys. Chem. 97*, 13668−13672.
30. Terazima, M., and Azumi, T. (1990) *Bull. Chem. Soc. Jpn. 63*, 741−745.
31. Yamaguchi, S., Hirota, N., and Terazima, M. (1998) *Chem. Phys. Lett. 286*, 284−290.
32. Devanathan, S., Pacheco, A., Ujj, L., Cusanovich, M., Tollin, G., Lin, S., and Woodbury, N. (1999) *Biophys. J. 77*, 1017−1023.
33. Van Brederode, M. E., Gensch, T., Hoff, W. D., Hellingwerf, K. J., and Braslavsky, S. E. (1995) *Biophys. J. 68*, 1101−1109.
34. Spiegel, D. R., Marshall, A. H., Jukam, N. T., Park, H. S., and Chang, T. (1998) *J. Chem. Phys. 109*, 267−274.
35. Kawahara, K., and Tanford, C. (1966) *J. Biol. Chem. 241*, 3228−3232.
36. Santoro, M. M., and Bolen, D. W. (1988) *Biochemistry 27*, 8063−8068.
37. Takeshita, K., Hirota, N., and Terazima, M. (2000) *J. Photochem. Photobiol. A 134*, 103−109.
38. Van Brederode, M. E., Hoff, W. D., Van Stokkum, I. H. M., Groot, M., and Hellingwerf, K. J. (1996) *Biophys. J. 71*, 365−380.
39. Cooper, A., Dixon, S. F., and Tsuda, M. (1985) *Eur. Biophys. J. 13*, 195−201.

40. Gensch, T., Strassburger, J. M., Gärtner, W., and Braslavsky, S. E. (1998) *Isr. J. Chem. 38*, 231−236.
41. Chalikian, T. V., and Breslauer, K. J. (1996) *Biopolymers 39*, 619−626.
42. Panick, G., Vidugiris, G. J. A., Malessa, R., Rapp, G., Winter, R., and Royer, C. A. (1999) *Biochemistry 38*, 4157−4164.
43. Landau, L., and Lifsitz, E. (1969) *Statistical Physics, Theoretical Physics*, Vol. 5, Pergamon Press, Oxford.
44. Heremans, K., and Smeller, L. (1998) *Biochim. Biophys. Acta 1386*, 353−370.
45. Zipp, A., and Kauzmann, W. (1973) *Biochemistry 12*, 4217−4228.
46. Wilkins, D. K., Gimshaw, S. B., Receveur, V., Dobson, C. M., Jones, J. A., and Smith, L. J. (1999) *Biochemistry 38*, 16424−16431.
47. Choi, J., Kim, H., and Lee, S. (1998) *J. Chem. Phys. 109*, 7001−7004.

BI0110600